ELSEVIER

Biophysical Chemistry 57 (1995) 55–64

Biophysical Chemistry

Brownian dynamics simulation of probe diffusion in DNA: effects of probe size, charge and DNA concentration

John D. Dwyer [a], Victor A. Bloomfield [b,*]

[a] *Department of Chemistry, College of St. Catherine, St. Paul, MN 55105, USA*
[b] *Department of Biochemistry, University of Minnesota, St. Paul, MN 55108, USA*

Abstract

We have used Brownian dynamics simulation to study probe diffusion in solutions of short chain DNA using our previously developed simulation algorithm [1]. We have examined the effect of probe size, charge, and DNA concentration on the probe diffusion coefficient, with the aim of gaining insight into the diffusion of proteins in a concentrated DNA environment. In these simulations, DNA was modeled as a worm-like chain of hydrodynamically equivalent spherical frictional elements while probe particles were modeled as spheres of given charge and hydrodynamic radius. The simulations allowed for both short range Lennard–Jones interactions and long ranged electrostatic interactions between charged particles. For uncharged systems, we find that the effects of probe size and DNA concentration on the probe diffusion coefficient are consistent with excluded volume models and we interpret our results in terms of both empirical scaling laws and the predictions of scaled particle theory. For charged systems, we observe that the effects of probe size and charge are most pronounced for the smallest probes and interpret the results in terms of the probe charge density. For an ionic strength of 0.1 M we find that, below a critical probe surface charge density, the probe diffusion coefficient is largely independent of probe charge and only weakly dependent on the DNA charge. These effects are discussed in terms of the interactions between the probe and the DNA matrix and are interpreted in terms of both the underlying physics of transport in concentrated solutions and the assumptions of the simulation model.

Keywords: Brownian dynamics; Probe diffusion; DNA; Polyelectrolytes; Macromolecular crowding; Electrostatics; Hydrodynamics

1. Introduction

Macromolecular diffusion in highly volume occupied solutions is a complicated process which depends both on the physical properties of the diffusing macromolecule and the properties of the matrix through which diffusion must take place. In order to understand the mechanisms of such transport processes (and ultimately the various biochemical processes dependent upon diffusional transport), it is necessary to understand the nature and relative significance of the many possible interactions between a diffusing macromolecule and its environment. Specific interactions which have been suggested to be important in this regard include direct excluded volume interactions [2,3], hydrodynamic interactions [4,5], long range electrostatic interactions [6,7], and steric interactions with anisotropic fibrous cytoplasmic structures such as microtubules [8,9].

* Corresponding author.

SSDI 0301-4622(95)00045-3

The development of a theoretical description of probe diffusion in concentrated solutions has been limited by the complexity of the problem. Several statistical mechanical theories which incorporate both direct excluded volume and hydrodynamic interactions for hard sphere systems have been developed [10–12]. While offering insight into the problem, the complexity and limited application of these theories has made experimental verification difficult.

In lieu of a formal theoretical treatment, semi-empirical scaling laws have been developed for describing probe diffusion as a function of the properties of both the polymer solution and the diffusing particle. The general form of these scaling laws is

$$\frac{D}{D_0} = \exp(-\alpha c^{\upsilon} R^{\delta}) \tag{1}$$

where D is the probe diffusion coefficient of a particle of radius R in a polymer solution of concentration c, and D_0 is the value of D at $c = 0$. Experiments on a wide range of polymer systems, both biological and synthetic [13–16], have demonstrated that such scaling laws can adequately describe probe diffusion over a wide range of solution concentrations. This work has led to some agreement as to the phenomenological ranges of α, υ, and δ as well as what factors affect these parameters. For example, υ typically falls in the range of 0.5 to 1.0, with the lower and upper limits being interpreted to reflect the relative contributions of hydrodynamic and direct interactions, respectively, to diffusional motion [8,14]. The parameter δ has been experimentally found to vary from 0 to 1. This variation, while partly due to experimental uncertainty, also reflects differences in the individual systems being studied. For example, Han and Hertzfeld [17] have shown using scaled particle theory that for spherical probe molecules the parameter δ increases and approaches 1 as the background polymer becomes more rod-like.

Although considerable experimental and theoretical work has been done on uncharged systems, less is known about the effects of electrostatic interactions on probe diffusion. Phillies [7] has shown that ionic strength I may be incorporated into the above scaling laws so that $\alpha \sim I^{\beta}$ with β in the range -0.5 to -0.167 for the diffusion of polystyrene in polyacrylic acid. Gorti and Ware [6] have also demonstrated an ionic strength dependence for the diffusion of polystyrene latex spheres in polysulfonic acid, although they found it to be quite weak. Odijk [18] has developed a limited scaling law for probe diffusion in polyelectrolyte solutions which predicts that β varies in the range -0.125 to -0.375 and that it scales with the polyelectrolyte charge density. The effect of the probe charge on its diffusion remains an unexplored question.

Because of the complexity of the interactions in these types of systems, interpretation of experimental results is difficult. Furthermore, practical considerations often make it impossible to carry out the kinds of experiments necessary to selectively control the various properties known to influence diffusion processes. In this paper we report on a series of Brownian dynamics simulations designed to systematically explore the effect of several of these properties on probe diffusion in concentrated DNA solutions. Our aim is to gain insight into the diffusion of proteins in a concentrated DNA environment. To accomplish this, we have employed our previously developed Brownian dynamics simulation algorithm [1] which allows for both direct excluded volume interactions and long range electrostatic interactions. Although this model is clearly approximate, we seek through these simulations to gain some insight into the physics underlying diffusion in these systems by examining the effects of probe size, charge, and background polymer (in our case, DNA) concentration on probe diffusion.

2. Methods

Simulations of probe diffusion in DNA were carried out using the model and methods which we have described previously [1]. Only a brief description of the model will be given here and the reader is referred to our original paper for more details.

We modeled DNA by 20 touching spherical frictional elements of radius 15.9 Å [19] to give a worm-like chain of contour length 636 Å, slightly more than the commonly accepted persistence length of 500 Å. Probe molecules were modeled as spheres of a given hydrodynamic radius. Brownian dynamics simulations of the resulting probe-DNA solutions were then carried out using the method of Ermak and

McCammon [20] in which particle displacements were governed by the equation

$$r_i(t+\tau) = r_i(t) + \frac{D_i\tau}{Kt}\sum_{j=1}^{N} F_{ij} + R_i(\tau) \qquad (2)$$

where D_i is the translational diffusion coefficient of particle i (probe or DNA segment), F_{ij} is the direct interparticle force between particles i and j, and $R_i(t)$ is a random displacement vector used to simulate solvent-mediated Brownian motion. For chain particles, the interparticle interaction potential was of the form

$$U_i = U_{\text{stretch}} + U_{\text{bend}} + U_{\text{LJ}} + U_{\text{DH}} \qquad (3)$$

where the first two terms represent harmonic intrachain stretching and bending potentials while the latter two terms describe interchain Lennard–Jones interactions (to ensure excluded volume) and long-range electrostatic interactions. The electrostatic interactions were modeled using the Debye–Hückel potential of the form

$$U_{\text{DH}} = C\frac{e^{\kappa a}}{1+\kappa a}\frac{e^{-\kappa r}}{r} \qquad (4)$$

where κ is the inverse Debye length, $C = q_i q_j e^2/\varepsilon k_B T$, and a is the radius of the particle. For probe molecules, the interaction potential included only the Lennard–Jones and Debye–Hückel terms. The force on a particle was then computed from the gradient of the potential.

Simulations were carried out employing periodic boundary conditions in a 700 Å box containing from 5 to 100 DNA chains (equivalent to a DNA concentration of 3–60 mg/ml) and 9 probe particles. Diffusion coefficients were determined using the mean squared particle displacement from the Brownian trajectory and the relationship

$$\langle r^2 \rangle = 6Dt \qquad (5)$$

Each simulation consisted of a series of 20–30 trajectories, with each trajectory consisting of 50 000 time steps. In Brownian dynamics simulations it is important that the time step be short enough so that interparticle forces remain essentially constant over the time step. We found that for this condition to be met, the size of the time step had to be shortened for the smaller probes: for probes of 20 Å or less, the time step was 5 ps while for larger probes a time step of 20 ps was used. Thus trajectories were 250 ns or 1 μs. Diffusion coefficients were calculated from mean squared particle displacements averaged over all trajectories and equivalent particles; uncertainties in calculated diffusion coefficients ranged from 10 to 15%.

Simulations were carried out on the Cray XMP-EA at the Minnesota Supercomputer Institute and on an IBM RS-6000. On the Cray, a 50 000 step trajectory required between 0.025 and 0.85 CPU hours depending upon DNA concentration.

3. Results and discussion

3.1. Uncharged systems

In order to test our simulation model and to assess the effects of probe size and DNA concentration on the probe diffusion coefficient without the complication of electrostatic interactions, we carried out a series of simulations in which all of the charges were switched off and only short-ranged Lennard–Jones interactions were calculated. The results of these simulations are shown in Fig. 1. As expected, for a given DNA concentration, D/D_0 is a decreasing function of probe size with the magnitude of the effect being dependent upon the DNA concentration. In order to fit these data to Eq. 1 using a minimum number of parameters, we have modified the equation so that $\alpha' = \alpha c^{\nu}$. The results of these fits are summarized in Table 1. While the uncertainties asso-

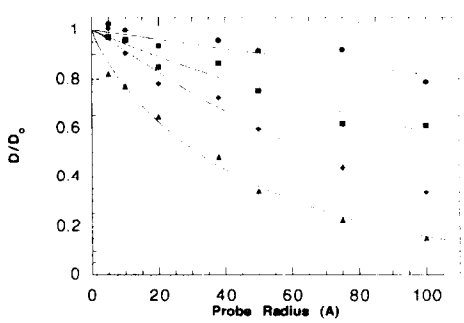

Fig. 1. Effect of probe radius on probe diffusion as a function of DNA concentration in the absence of electrostatic interactions. [DNA] = 3 mg/ml (●); 15 mg/ml (■); 30 mg/ml (♦); and 60 mg/ml (▲). Solid lines represent best fit of simulation data to Eq. 1.

ciated with the fitted parameters α' and δ are relatively high, the data suggest that α' is an increasing function of the DNA concentration while δ is constant and approximately equal to 1. This dependence of α' on c is consistent with its definition while the $\delta = 1$ dependence is consistent with both previous experimental results for probe diffusion in rods and theories based on excluded volume effects.

In Fig. 2, we have replotted this data to show the effect of DNA concentration. In Fig. 2a, D/D_0 is plotted against DNA concentration for the various probe sizes. Here we observe D/D_0 to be a decreasing function of DNA concentration with the magnitude of this dependence increasing with increasing probe size. These data have been fit to Eq. 1 modified so that $\alpha'' = \alpha R^{\delta}$ (again to reduce the number of fitted parameters) and the results summarized in Table 1. In this case, we find α'' to be an increasing function of R (consistent with its definition) while v is generally about 1 with some indication that it may be slightly decreasing for the largest probe sizes. The $v = 1$ behavior is in accord with the absence of hydrodynamic interactions in these simulations and previous experiments on similar systems.

Finally, Han and Hertzfeld [17], in an extension of the scaled particle theory of Muramatsu and Minton [21], have developed a model for diffusion of spherical probes in an isotropic solution of spherocylinders. According to their model, the probe diffusion coefficient depends on the probe size according to

$$\frac{D}{D_0} = \exp\left(-\left(\frac{\Delta r}{R}\right)\xi\right) \qquad (6)$$

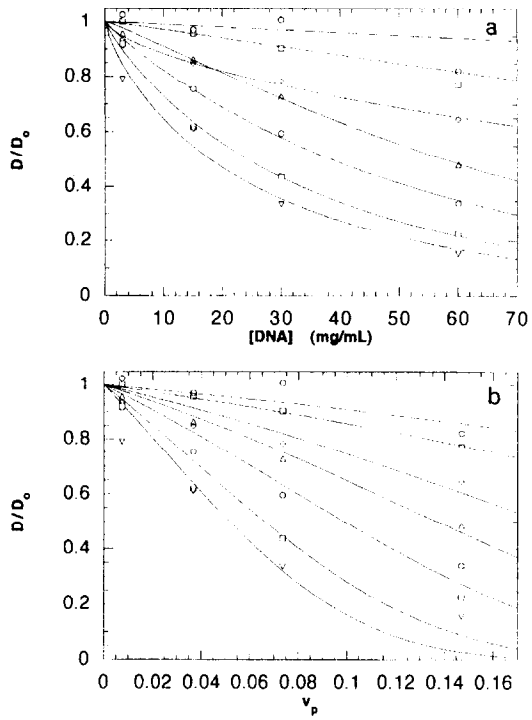

Fig. 2. (a) Effect of [DNA] on probe diffusion as a function of probe size (R) in the absence of electrostatic interactions. $R = 5$ Å (○); 10 Å (□); 20 Å (◇); 38 Å (△); 50 Å (○, with dot); 75 Å (□, with dot); and 100 Å (▽). Solid lines represent best fit of simulation data to equation 1. (b) Same as (a) except plotted against the volume fraction DNA. Solid lines are best fits of data to Eq. 6.

where $\Delta r/R$ is a relative step size and ξ is a function of the probe radius R, the length of the spherocylinders (i.e., DNA chains), the radius of the spherocylinders, and the volume fraction v_p of the

Table 1
Scaling law parameters for uncharged systems

[DNA]	α' [a]	δ [a]	R (Å)	α'' [b]	v [b]	$\Delta r/R$ [c]
3.0	0.002	1.01	5	0.001	1.01	3.80
15.0	0.006	0.95	10	0.002	1.09	2.32
30.0	0.006	1.09	20	0.025	0.69	1.43
60.0	0.037	0.84	38	0.006	1.14	0.63
			50	0.022	0.94	0.58
			75	0.042	0.88	0.43
			100	0.072	0.78	0.32

[a] Data from Fig. 1 fit to $D/D_0 = \exp(-\alpha' R^{\delta})$.
[b] Data from Fig. 2a fit to $D/D_0 = \exp(-\alpha'' c^{v})$.
[c] Data from Fig. 2b fit to $D/D_0 = \exp[-(\Delta r/R)\xi]$.

solution occupied by the spherocylinders. In Fig. 2b we have replotted our data in this form and have fit it to the above equation using 15.9 Å for the radius of our DNA chains and 636 Å for the length of the chains in order to calculate v_p and ξ. We find that the agreement between theory and our simulations is quite good for the smaller probe sizes with discrepancies increasing with increasing probe size. We do not find the fitted parameter, $\Delta r/R$, to have the constant value 2/3 as predicted by Han and Hertzfeld. The discrepancies between the theory and the simulations for the larger probes is expected in light of the fact that scaled particle theory tends to overestimate the obstruction effect on diffusion as the probe size approaches that of the background chains. Furthermore, the scaling law of Langevin and Rondelez [22] predicts that in the limit of increasing probe size D/D_0 should approach a limit governed by the solution viscosity. This behavior has been experimentally confirmed by Tracy and Pecora for a rod-sphere system [23].

3.2. Charged systems

To examine the effects of probe charge and size on the probe diffusion coefficient we have carried out two sets of simulations in which the probe charge was set to +10 and −10. The net charge on the DNA chains was calculated assuming 80% charge neutralization due to monovalent counterions [24]; thus each bead in the DNA worm-like chains was given a charge of −4.0. All simulations were carried out at an ionic strength of 0.1 M.

The results of these simulations are shown in Fig. 3. As with the uncharged systems, these data again show that D/D_0 is a decreasing function of DNA concentration. However, probe size and charge strongly influence this dependence. In particular, it can be seen that above a certain critical probe radius (approximately 20 Å), D/D_0 is essentially independent of the probe charge. For the smaller probes, the effect of probe size depends strongly on whether the probe has the same (negative) or opposite (positive)

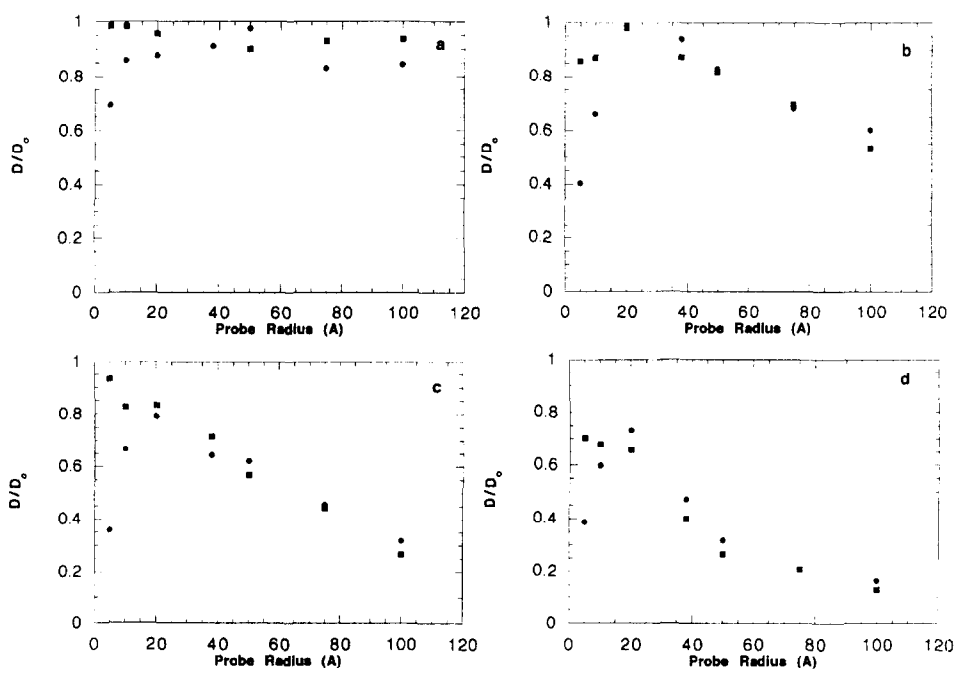

Fig. 3. Effect of probe radius on probe diffusion as a function of DNA concentration for probes with charge +10 (●) and −10 (■) in 0.1 M monovalent salt. Panels (a)–(d) are for [DNA] = 3, 15, 30, and 60 mg/ml.

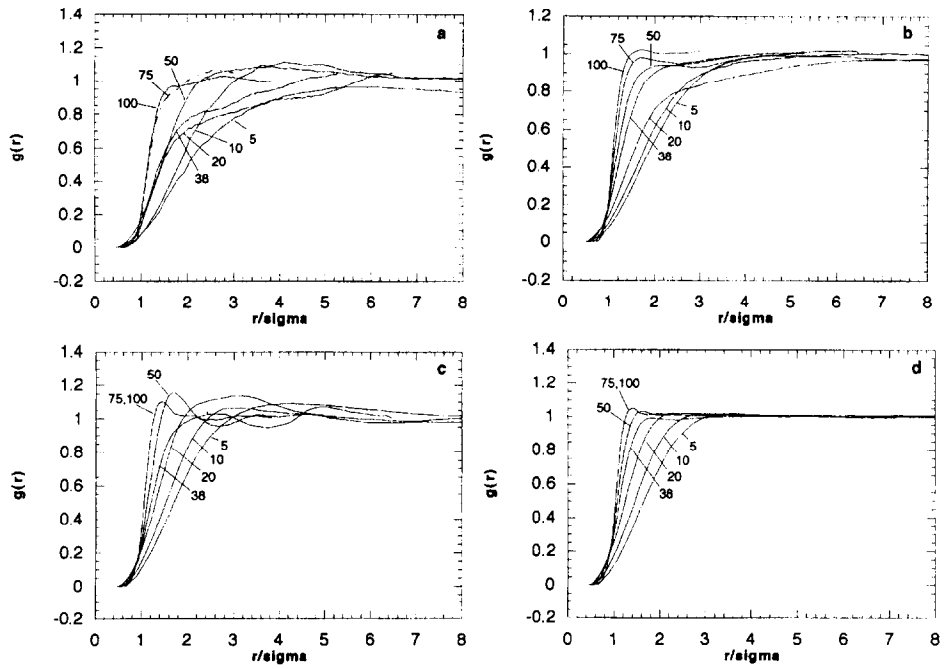

Fig. 4. Probe–chain radial distribution functions for negatively charged probes ($q_{probe} = -10$) as a function of DNA concentration and probe radius (R) for $I = 0.1$ M monovalent salt. Panels (a)–(d) are for [DNA] = 3, 15, 30, and 60 mg/ml. Curves are labeled with the probe radius (in Å).

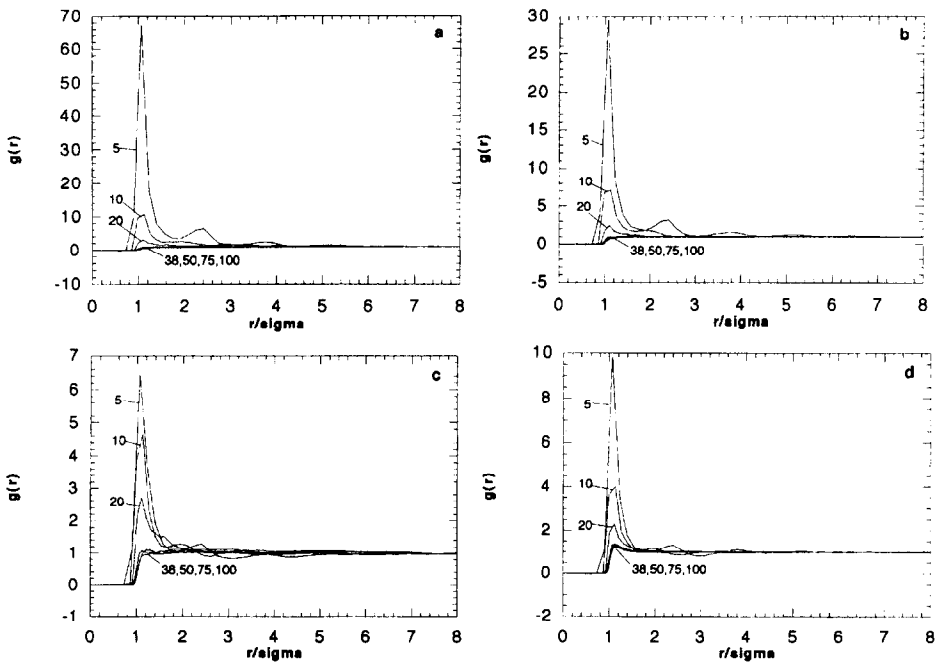

Fig. 5. Probe–chain radial distribution functions for positively charged probes ($q_{probe} = +10$) as a function of DNA concentration and probe radius (R) for $I = 0.1$ M monovalent salt. Panels (a)–(d) are for [DNA] = 3, 15, 30, and 60 mg/ml. Curves are labeled with the probe radius (in Å).

charge as that of the DNA. It is noted, particularly at the higher DNA concentrations, that unlike the uncharged system D/D_0 does not appear to extrapolate to 1 in the limit of zero size. Negatively charged probes show a continued increase in D/D_0 with decreasing probe size, while positively charged probes show a decrease.

This behavior is a reflection of the simulation model in which a constant charge is maintained for the different sized probes, thus varying the surface charge density. For the probes used in these simulations, the surface charge density varied from ± 0.0318 Å^{-2} for the smallest probes to $\pm 7.96 \cdot 10^{-5}$ Å^{-2} for the largest. The larger surface charge densities are approximately those of small (1–3 Å) singly and doubly charged ions. To further explore this behavior, we have computed the probe-chain radial distribution function $g(r)$ for these simulations and plotted the results in Figs. 4 and 5. Here, r is the computed center-to-center distance between the probe particles and the individual spherical segments which constitute the worm-like DNA chains. For the negatively charged probes (Fig. 4), increasing probe size results in a shift of the radial distribution function to smaller values of r/σ (where r is the center-to-center separation distance and σ is the contact separation) in turn reflecting the decrease in the magnitude of the repulsive interaction between the probe and the DNA lattice. In fact, at the higher DNA concentrations, peaks in the radial distribution function (indicative of structuring in the solution) are seen for the larger probes. We interpret this as a further reflection of the decreased surface charge density of the larger probes and the increased steric constraints imposed by the higher DNA concentrations.

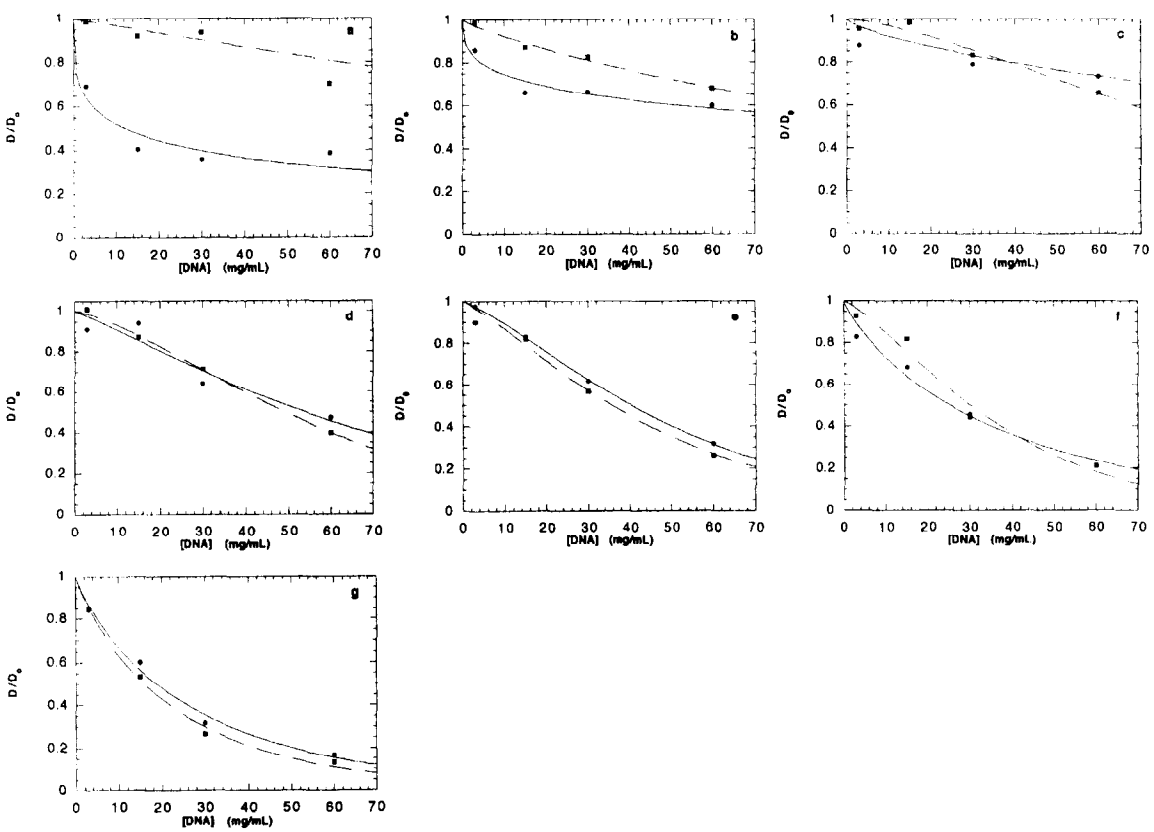

Fig. 6. Effect of [DNA] on probe diffusion as a function of probe radius (R) for probes with charge +10 (●) and −10 (■) in 0.1 M monovalent salt. Panels (a)–(g) are for $R = 5$, 10, 20, 38, 50, 75, and 100 Å. The lines represent the best fits of the data to Eq. 1.

For the positively charged probes (Fig. 5), the radial distribution functions show the opposite behavior. The smallest probes show strongly peaked radial distribution functions consistent with the strong electrostatic attraction between the probe and the DNA matrix. As the probe increases in size the electrostatic interaction weakens and approaches the behavior of the negatively charged probes. While this behavior is qualitatively repeated at all of the DNA concentrations, it is noted that the magnitude of the attractive potential experienced by the smaller probes (reflected by the peak height in the radial distribution function) decreases with increasing DNA concentration up to 30 mg/ml and then slightly increases. This latter increase likely reflects the onset of increased packing constraints brought on by the higher DNA concentration.

We have estimated the distance of closest approach between the probe and the DNA chains from these radial distribution functions as the value of r/σ at which $g(r) = 0.5$. From this we have determined the corresponding surface to surface separation between the probe and the chains. We find that for the positively charged probes the surface to surface separation varies smoothly from 0 to 7 Å with increasing probe size, and depends only slightly on DNA concentration. The surface to surface separation for the negatively charged probes decreases with increasing probe size from about 15–20 Å down to 5–10 Å for the largest probe. Thus as the probe size is increased and the surface charge density is decreased, the surface-to-surface separation approaches a constant value for both probe charges, consistent with the observed behavior of D/D_0 seen in Fig. 3. In the limit of small probe size, the surface separation approaches contact for positively charged probes suggesting that these probes are electrostatically trapped within the DNA matrix. That is, the size of the local cavity in the matrix within which the probe may diffuse is decreased due to the strong attractive electrostatic potential created by the probe. As this cavity size decreases (with increasing probe charge density) the diffusional motion of the probe is expected to be limited by the diffusion of the chains, exactly the behavior seen in Fig. 3.

The behavior of the negatively charged probes with decreasing probe size is rather more complicated but can be at least qualitatively understood again in terms of probe size, charge density, and DNA concentration. Decreasing the probe size should increase D/D_0 while the corresponding increase in the surface charge density should serve to decrease D/D_0 due to the stronger repulsion from the DNA matrix. To first order, these effects offset each other so that in the limit of small probe sizes, D/D_0 should approach a constant value. Furthermore, this value will be limited by the steric constraints of the DNA matrix and so would be expected to decrease with increasing DNA concentration.

In Fig. 6 we have replotted the data of Fig. 3 so that the probe size (and thus charge density) is held constant to examine the dependence of probe diffusion on the DNA concentration. For all but the smallest two probes, we observe (Fig. 6c–g) that the effect of the DNA concentration on the probe diffusion coefficient is, within the uncertainty of our results, independent of the sign of the charge on the probe. In fact, comparison of the data in Fig. 6 to those in Fig. 2a shows that the dependence of D/D_0 on DNA concentration appears to be only weakly dependent on electrostatic interactions and then only for the smaller probes. Again, we believe this reflects the assumptions of the simulation model. As the probes increase in size their surface charge density decreases and thus the magnitude of their electrostatic interaction with the DNA matrix decreases. A similar insensitivity of D/D_0 to the nature (attractive or repulsive) of weak long range interactions was observed by Abney et al. [25] in their simulations of protein self diffusion in membranes. Furthermore, we have found that, at the 0.1 M ionic strength at which these simulations were carried out, the DNA self diffusion coefficient, while dependent upon the DNA concentration, is largely insensitive to electrostatic interactions. Thus with increasing size and decreasing electrostatic interactions, the probe diffusion coefficient is expected to approach the chain diffusion coefficient which, as noted above, is largely independent of electrostatic interactions.

For the two smallest probes (Fig. 6a and b), the dependence of D/D_0 on DNA concentration is considerably more pronounced owing to the strong electrostatic interactions. The strong repulsion of the negatively charged probes results in retardation of probe diffusion (relative to the uncharged system) and may be understood in terms of a larger effective

probe size afforded by a repulsive ion atmosphere surrounding the probe whose thickness depends on both the charge density of the probe (thus its radius) and the solution ionic strength. Thus the smallest probes are relatively more hindered than the larger ones with this effect diminishing with increasing probe size.

We have suggested that the attractive potential generated by the small positively charged probes results in a reduction in the size of the local cavity within the matrix within which they must diffuse. For this to occur, it may reasonably be assumed that the DNA concentration needs to be high enough so that the DNA chains significantly overlap, i.e., within the semi-dilute concentration regime. The lower boundary for this concentration regime has been estimated by Wang et al. [26] to be 10–20 mg/ml at high salt for DNA fragments of one persistence length (similar to those used in these simulations). The results of Fig. 6a and b for the positively charged probes show that D/D_0 decreases rapidly with increasing DNA concentration and then levels off above about 20 mg/ml. These data therefore suggest that with the onset of the semi-dilute regime, the strong electrostatic attraction of these probes for DNA and the high local chain segment density results in an essentially constant and relatively hindered environment in which the probe must diffuse. Diffusion is then limited by the rate at which this local environment relaxes, which depends in turn on the rate of diffusion of the chains themselves.

Finally, we have fit the data in Fig. 6 to Eq. 1 (again modified so that $\alpha'' = \alpha R^{\delta}$ in order to quantify these effects in terms of the parameters α'' and υ. The results of these fits are summarized in Table 2. For the negatively charged probes, both the α'' and υ parameters behave similarly to what was seen in the uncharged system. This is consistent with the model in which the repulsive interactions between the probe and the DNA matrix may be treated in terms of an effective probe size which includes a repulsive ion atmosphere. The results for the positively charged probe suggest that both α'' and υ depend on the probe charge density. To our knowledge, the effect of probe charge density on these parameters has not been previously characterized experimentally or theoretically. Although our data are probably not good enough to explore this dependence analytically, they do suggest that probe charge density be taken into account in interpretation of the experimental values of these parameters.

Table 2
Scaling law parameters for charged systems [a]

	Probe charge = +10		Probe charge = −10	
R (Å)	α''	υ	α''	υ
5	0.32	0.32	0.003	1.03
10	0.13	0.34	0.0008	0.86
20	0.016	0.73	0.0011	1.46
38	0.0065	1.17	0.0026	1.43
50	0.0057	1.29	0.0083	1.24
75	0.045	0.85	0.0097	1.31
100	0.057	0.85	0.062	0.87

[a] Data from Fig. 6 fit to $D/D_0 = \exp(-\alpha'' c^{\upsilon})$.

4. Conclusions

These simulations confirm that diffusion of neutral probe molecules in a solution of uncharged rods depends on both the probe radius and rod concentration. We have shown that these dependencies may be described by a stretched exponential scaling law of the form of Eq. 1 with the parameters δ and υ on order of unity. We have also shown that our simulation results are consistent with the predictions of scaled particle theory when the ratio of the rod length to probe radius is large.

For diffusion of charged probes in a solution of charged DNA, we observe that the dependence of probe diffusion coefficient upon probe size and DNA concentration is modified by both the sign and magnitude (i.e., charge density) of the probe. At charge densities corresponding to those found on typical proteins, we find that charge effects are minimal at the approximately physiological ionic strengths used in these simulations and that probe diffusion is dependent on the probe radius and DNA concentration in much the same manner observed for uncharged systems. However, for charge densities comparable to those of small ions, we find probe diffusion to be strongly influenced by charge effects with both like and oppositely charged probes showing reduced mobility relative to the same probe in the uncharged system. While such high uniform charge densities

are unrealistic for proteins except at extremes of pH, it is possible for proteins to have patches with charge densities of comparable magnitude and thus be susceptible to similar interactions with a charged background matrix. In particular, we have argued that the strong attractive interaction seen between the small positively charged probes and the DNA in these simulations results in something which may be viewed as analogous (but not equivalent to) binding between the probe and the DNA. A protein with a high local charge density may interact with neighboring DNA segments in a similar, but asymmetric, manner and, given the discrete charge density on an actual DNA chain, lead to a true binding interaction. In this way, it may be that protein local charge density constitutes the primary basis for non-specific protein–DNA interactions.

Acknowledgements

This work was partially supported by NSF grant DMB9105910. We thank Professor Norma Allewell and Dr. Himanshu Oberoi for access to the IBM RS-6000. Supercomputer time was provided under a grant from the Minnesota Supercomputer Institute.

References

[1] J.D. Dwyer and V. A. Bloomfield, Biophys. J., 65 (1994) 1810–1816.
[2] A.G. Ogston, Faraday Soc. Trans., 54 (1958) 1754.
[3] A.G. Ogston, B.N. Preston and J.D. Wells, Proc. R. Soc. London A, 333 (1973) 297–316.
[4] R.I. Cukier, Macromolecules, 17 (1984) 252–255.
[5] A.R. Altenberger and M. Tirrell, J. Chem. Phys., 80 (1984) 2208–2213.
[6] S. Gorti and B.R. Ware, J. Chem. Phys., 83 (1985) 6449–6456.
[7] G.D.J. Phillies, T. Pirnat, M. Kiss, N. Teasdale, D. Maclung, H. Inglefield, C. Malone, A. Rau, L.P. Yu and J. Rollings, Macromolecules, 22 (1989) 4068–4075.
[8] L. Hou, F. Lanni and K. Luby-Phelps, Biophys. J., 58 (1990) 31–43.
[9] K. Jacobson and J. Wojcieszyn, Proc. Natl. Acad. Sci. USA, 81 (1984) 6747–6751.
[10] S Hanna, W. Hess and R. Klein, Physica, 111A (1982) 181–199.
[11] P. Mazur and W. van Saarloos, Physica, 115A (1982) 21–57.9.
[12] C.W.J. Beenakker and P. Mazur, Physica, 126A (1984) 349–370.
[13] G.D.J. Phillies, Macromolecules, 19 (1986) 2367–2376.
[14] M.A. Tracy and R. Pecora, Macromolecules, 25 (1992) 337–349.
[15] M. R. Wattenbarger, V.A. Bloomfield, Z. Bu and P. Russo, Macromolecules, 25 (1992) 5263–5265.
[16] L. Hou, F. Lanni and K. Luby-Phelps, Biophys. J., 58 (1990) 31–43.
[17] J. Han and J. Hertzfeld, Biophys. J., 65 (1993) 1155–1161.
[18] T. Odijk, Macromolecules, 12 (1979) 688–693.
[19] P.J. Hagerman and B.H. Zimm, Biopolymers, 20 (1981) 1481–1502.
[20] D.L. Ermak and J.A. McCammon, J. Chem. Phys., 69 (1978) 1353–1360.
[21] N. Muramatsu and A.P. Minton, Proc. Natl. Acad. Sci. USA, 85 (1988) 2984–2988.
[22] D. Langevin and F. Rondelez, Polymer, 19 (1978) 875–882.
[23] M.A. Tracy and R. Pecora, Macromolecules, 26 (1993) 1862–1868.
[24] G.S. Manning, Acc. Chem. Res., 12 (1979) 443–449.
[25] J.R. Abney, B.A. Scalettar and J.C. Owicki, Biophys. J., 55 (1989) 817–833.
[26] L. Wang, M.M. Garner and H. Yu, Macromolecules, 24 (1991) 2368–2376.